

Temporal boundaries in electromagnetic materials

Jonathan Gratus^{1,2,*}, Rebecca Seviour^{3,†}, Paul Kinsler^{1,2,4,‡} and Dino A. Jaroszynski^{2,5,§}

¹ Department of Physics, Lancaster University, Lancaster LA1 4YB, United Kingdom,

² The Cockcroft Institute, Sci-Tech Daresbury, Daresbury WA4 4AD, United Kingdom,

³ University of Huddersfield, Huddersfield HD1 1JB, United Kingdom,

⁴ Department of Physics, Imperial College London, Prince Consort Road, London SW7 2AZ, United Kingdom. and

⁵ Department of Physics, SUPA and University of Strathclyde, Glasgow G4 0NG, United Kingdom.

Temporally modulated optical media are important in both abstract and applied applications, including time crystals, spacetime transformation optics, and dynamically controllable metamaterials. Here we investigate the behaviour of temporal boundaries, an important component in time crystals, and which have a range of potentially exotic properties. We show that traditional approaches based on an assumption of constant dielectric properties, with loss incorporated as an imaginary part, lead necessarily to unphysical solutions. Further, although physically reasonable predictions can be recovered using a narrowband approximation, here we show that the most appropriate models use materials with a temporal response and dispersive behaviour.

Boundaries play a key role in physical models; they provide initial and final states in dynamical systems, constrain analytic solutions in confined systems, and represent transitions between different modes of operation. Research into temporal boundaries dates back to the 1950s. Morgenthaler [1] demonstrated a temporal change of the permittivity produces both forward and backward propagating waves; a result echoed in modern directional formulations for wave propagation [2–6]. Temporal boundaries can act as a time-reversing mirror in acoustics [7], and in electromagnetism an instantaneous time mirror with a sign-change in permittivity has been predicted [8] to cause field amplification. Other examples include dynamically configurable system [9, 10], spacetime transformation devices [11–14], or, more recently, concepts such as spacetime crystals [15] and “field patterns” [16].

Here we show that modelling loss using a constant complex permittivity and permeability [8, 17–19] is physically incompatible with a temporal boundary. Our conclusion is very significant for technological applications of temporal boundaries, because in experimental contexts loss is frequently expressed as the electric loss tangent (“ $\tan \delta$ ”), based on the ratio between the imaginary and real parts of the permittivity; i.e. is *defined* by properties and assumptions that cannot be trusted. Such simplistic models can lead to unphysical post-boundary solutions that grow exponentially, despite being applied to passive and lossy material; or may become complex-valued despite being real-valued beforehand.

In this article the term “boundary” refers to an interface between two regions with different constitutive relations (CRs). In electromagnetism CRs are most simply given by a permittivity ϵ and permeability μ , although more complicated CRs are also allowed. In contrast to spatial boundary conditions that describe the interface between two different static media, here we consider a temporal boundary at $t = t_b$, where the medium has one set of CR properties before the transition ($t < t_b$), and different CRs afterwards ($t > t_b$). In our idealised transition, the CR for the entire region changes instantaneously; although gradual transitions are also possible [20, 21]. The unphysical consequences arise irrespective of which of the two possible types of temporal boundary con-

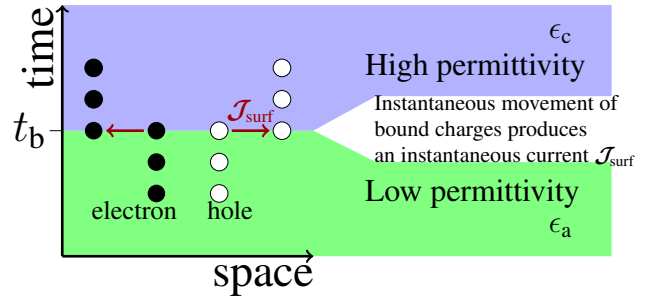


FIG. 1: A temporal boundary or transition based on fundamental TBCs. Here, a sudden increase of permittivity at $t = t_b$, represented as the movement of bound charges, necessarily generates a microscopic “time-surface” current $\mathcal{J}_{\text{surf}}$.

dition (TBC) we consider. The first, or “natural” TBC [22], is derived from Maxwell’s equations on the assumption that all the *currents* are finite, which leads to the continuity of \mathbf{B} and \mathbf{B} . The second “fundamental” TBC is motivated by treating only \mathbf{E} and \mathbf{B} as physical EM fields, with \mathbf{D} and \mathbf{H} as derived fields acting as a gauge for the current [23–25]; here \mathbf{E} and \mathbf{B} are also continuous, but a *temporal-surface* dipole current appears at the transition.

After demonstrating and defining the problem, we present two methods for obtaining physically meaningful solutions. The first applies the constant complex CR model whilst using a narrow band approximation (NBA). This leads to a solution based on complex conjugate pairs of frequencies and refractive indices. Although partially successful, this demonstration merely hides the fact that to model lossy media correctly when there is a temporal boundary, one requires a time-dependent material response, and therefore dispersive CR, where ϵ and/or μ depend on frequency. Besides, just as a dynamic medium model requires its own fields to represent its state, in the frequency domain we see that a dispersive medium supports one or more additional modes; and this necessary information cannot be included in the standard constant complex CR model. Thus in either time or frequency, additional boundary conditions (ABCs) must be specified.

Note that proofs and additional discussion is presented in the Supplementary Material.

In *Linear Media* any EM field can be represented in the Fourier domain by a sum or integral of terms of the form $\exp(-i\omega t + i\mathbf{k} \cdot \mathbf{x})$, where $\omega \in \mathbb{C}$ is a complex frequency, and $\mathbf{k} \in \mathbb{C}^3$ a complex wavevector. Since the source free Maxwell's equations (5) are linear, with $\mathbf{J}_{\text{total}} = 0$ and $\rho = 0$, it is sufficient to consider just a single mode

$$E_x(t, z) = E_0 \exp(-i\omega t + ikz) \quad \text{where} \quad k, \omega \in \mathbb{C}, \quad (1)$$

with \mathbf{k} oriented along the z -axis (along \hat{z}), and \mathbf{E} along \hat{x} .

Now consider a temporally dispersive medium where the CRs are given with permittivity $\tilde{\epsilon}(-\omega)$ and permeability μ_0 . The negative sign in the argument to $\tilde{\epsilon}$ is a consequence of choosing the form $e^{-i\omega t}$. If ω and $\tilde{\epsilon}(-\omega)$ are both real then $\tilde{\epsilon}(-\omega)$ can be replaced with $\tilde{\epsilon}(\omega)$; but this not allowed in our following calculations, because extra care must be taken when using complex permittivity to model damping. From Maxwell (5) we obtain a dispersion relation, and define the refractive index[26–28]. These are

$$k^2 - \omega^2 \mu_0 \tilde{\epsilon}(-\omega) = 0, \quad (2)$$

$$\tilde{n}(-\omega)^2 = c_0^2 \mu_0 \tilde{\epsilon}(-\omega), \quad (3)$$

where $c_0 = (\epsilon_0 \mu_0)^{-1/2}$ is the vacuum speed of light.

We now ask whether these CRs correspond to a passive lossy medium, i.e. one dampened with no external energy added. Given that both ω and k can be either real or complex, there are two possibilities that are straightforward to consider. These fit into the temporally propagated and spatially propagated viewpoints respectively [29], and are:

First, if ω is real and positive, we require that plane waves are spatially evanescent in the propagation direction, which implies $\text{Im}(\tilde{\epsilon}(-\omega)) > 0$.

Second, if k is real, then we need $\text{Im}(\omega) < 0$ to damp the field, leading to the requirement that when $\omega^2 \tilde{\epsilon}(-\omega)$ is real and positive, then $\text{Im}(\omega) < 0$.

How the fields represented by these modes, change as they cross a temporal boundary will depend on how the change in CRs is specified, and on the chosen TBCs.

Temporal Boundary Conditions: Two types of electromagnetic TBC can be identified, both originating from choices about bound currents representing the material response. First, as depicted in Fig. 1, we could identify the sudden change in the CRs at $t = t_b$ as leading to an instantaneous *temporal-surface* dipole current ($\mathcal{J}_{\text{surf}}$). The total current, $\mathbf{J}_{\text{total}}$, in the medium is

$$\mathbf{J}_{\text{total}} = \mathbf{J}_{\text{reg}} - \delta(t - t_b) \mathcal{J}_{\text{surf}}, \quad (4)$$

where \mathbf{J}_{reg} is the usual finite current in Maxwell's equations:

$$\begin{aligned} \nabla \cdot \mathbf{B} &= 0, \quad \nabla \cdot \mathbf{D} = \rho \\ \nabla \times \mathbf{E} + \partial_t \mathbf{B} &= 0 \quad \text{and} \quad \nabla \times \mathbf{H} - \partial_t \mathbf{D} = \mathbf{J}_{\text{total}}. \end{aligned} \quad (5)$$

Since the fields $\mathbf{E}, \mathbf{B}, \mathbf{D}, \mathbf{H}$ may be discontinuous we write

$$\mathbf{D}(t, \mathbf{x}) = \theta(t_b - t) \mathbf{D}_a(t, \mathbf{x}) + \theta(t - t_b) \mathbf{D}_c(t, \mathbf{x}) \quad (6)$$

where \mathbf{D}_a and \mathbf{D}_c are the \mathbf{D} before and after the transition. Using (4) and (6) in the Maxwell-Ampère equation, we have

$$\begin{aligned} \mathbf{J}_{\text{total}} &= \mathbf{J}_{\text{reg}} - \delta(t - t_b) \mathcal{J}_{\text{surf}} = \nabla \times \mathbf{H} - \partial_t \mathbf{D} \\ &= \theta(t_b - t) \nabla \times \mathbf{H}_a(t, \mathbf{x}) + \theta(t - t_b) \nabla \times \mathbf{H}_c(t, \mathbf{x}) \\ &\quad - \theta(t_b - t) \partial_t \mathbf{D}_a(t, \mathbf{x}) - \theta(t - t_b) \partial_t \mathbf{D}_c(t, \mathbf{x}) \\ &\quad - \delta(t - t_b) \{ \mathbf{D}_c(t, \mathbf{x}) - \mathbf{D}_a(t, \mathbf{x}) \}. \end{aligned}$$

This approach can also be used for \mathbf{B} in the Maxwell-Faraday equation to derive a similar result. The TBC are

$$[\mathbf{D}] = \mathcal{J}_{\text{surf}} \quad \text{and} \quad [\mathbf{B}] = 0, \quad (7)$$

where $[\mathbf{D}] = \mathbf{D}_c(t_b, \mathbf{x}) - \mathbf{D}_a(t_b, \mathbf{x})$, etc. One option [1, 8] is to set $\mathcal{J}_{\text{surf}} = 0$, to obtain the *natural* TBC, i.e.

$$[\mathbf{D}] = 0 \quad \text{and} \quad [\mathbf{B}] = 0. \quad (8)$$

Alternatively, if treating \mathbf{E} and \mathbf{B} as the only physical fields, we get the *fundamental* TBC, i.e.

$$[\mathbf{E}] = 0 \quad \text{and} \quad [\mathbf{B}] = 0, \quad (9)$$

which rely on (7) to calculate the conserved temporal-surface current $\mathcal{J}_{\text{surf}}$. This is an analogous approach to that describing the surface current around a permanent magnet [23].

Constant Complex CR gives Unphysical Results: Even a time boundary between a vacuum with $\epsilon = \epsilon_0$ and a lossy medium with $\epsilon = \epsilon_c$, where ϵ_c is a non real constant with $\text{Im}(\epsilon_c) < 0$ and $\text{Re}(\epsilon_c) > 0$, results in a failure. For simplicity, we set $t_b = 0$, so that $\mathbf{D}(t, \mathbf{x}) = \epsilon_0 \mathbf{E}(t, \mathbf{x})$ for $t < 0$, and $\mathbf{D}(t, \mathbf{x}) = \epsilon_c \mathbf{E}(t, \mathbf{x})$ for $t > 0$; and then choose a field polarization so that $\mathbf{E} = E_x(t, z)\hat{x}$, and $\mathbf{B} = B_y(t, z)\hat{y}$.

Pre-boundary ($t < 0$), we start with a single real mode

$$E_x(t, z) = E_0 \cos(\omega_a t - k_a z), \quad (10)$$

with $E_0 \in \mathbb{R}$ and $B_y(t, z) = E_x/c_0$. Here ω_a, k_a are both real and positive and satisfy the vacuum dispersion relation $c_0^2 k_a^2 = \omega_a^2$. Since the post-boundary lossy material, with ω_c and k_c , must have $\text{Im}(\epsilon_c) > 0$, the $t > 0$ general solution is

$$\begin{aligned} E_x(t, z) &= (g_+^- e^{-i\omega_c t + ik_c z} + g_-^- e^{-i\omega_c t - ik_c z} \\ &\quad + g_+^+ e^{i\omega_c t - ik_c z} + g_-^+ e^{i\omega_c t + ik_c z}), \\ B_y(t, z) &= \frac{k_c}{\omega_c} (g_+^- e^{-i\omega_c t + ik_c z} - g_-^- e^{-i\omega_c t - ik_c z} \\ &\quad + g_+^+ e^{i\omega_c t - ik_c z} - g_-^+ e^{i\omega_c t + ik_c z}), \end{aligned} \quad (11)$$

with the dispersion relation

$$k_c c_0 = n_c \omega_c \quad \text{where} \quad n_c = c_0(\epsilon_c \mu_0)^{1/2}. \quad (12)$$

The choice of root for n_c is unimportant, as both roots are included in (11). The first root $\text{Re}(n_c) > 0$, since $\text{Im}(\epsilon_c) > 0$, requires $\text{Im}(n_c) > 0$; and the second root $\text{Re}(n_c) < 0$ with $\text{Im}(n_c) < 0$. Applying the fundamental TBC (9), just before the time boundary, we have

$$E_x(0^-, z) = \frac{1}{2} E_0 (e^{ik_a z} + e^{-ik_a z}), \quad (13)$$

and $B_y(0^-, z) = (k_a/\omega_a)E_x$. Just after the time boundary

$$\begin{aligned} E_x(0^+, z) &= (g_-^+ + g_-^-) e^{-ik_c z} + (g_+^+ + g_+^-) e^{ik_c z}, \\ B_y(0^+, z) &= \frac{k_c}{\omega_c} [(g_-^+ - g_-^-) e^{-ik_c z} + (g_+^- - g_+^+) e^{ik_c z}]. \end{aligned} \quad (14)$$

Note that except for different constants, the result is the same as would be obtained using the natural TBC (8).

From (13) and (14) we see that $k_c = k_a$ or $k_c = -k_a$ must hold and $\omega_c = n_a \omega_a / n_c$. We can choose $k_c = k_a$ without affecting the analysis, so the four unknowns can be rearranged to yield,

$$g_-^+ = g_+^- = \frac{1}{4} E_0 (1 + n_c) \quad \text{and} \quad g_-^- = g_+^+ = \frac{1}{4} E_0 (1 - n_c). \quad (15)$$

In general, for $t > 0$ all the g_{\pm}^{\pm} coefficients of $E_x(t, z)$ are non zero. Let $c_c = c_R + i c_I = c_0 / n_c$ then $c_R > 0$ and $c_I < 0$, and expand (11) to yield

$$\begin{aligned} E_x(t, z) &= g_-^- e^{ik_c(-c_R t + z)} e^{k_c c_I t} + g_-^- e^{ik_c(-c_R t - z)} e^{k_c c_I t} \\ &\quad + g_-^+ e^{ik_c(c_R t - z)} e^{-k_c c_I t} + g_+^+ e^{ik_c(c_R t + z)} e^{-k_c c_I t}. \end{aligned} \quad (16)$$

Now we have $k_c = k_a > 0$ and $c_I < 0$, so E increases exponentially with time *despite* this being a lossy medium. Clearly this is physically invalid, so the constant complex CR model has *failed*. Further, substituting (15) into (16) we observe that in general $E_x(t, z)$ is complex valued. This, despite the TBC (9) and the initial field (10) being real-valued. This is because the differential equation for the medium when $t > 0$ (following from (5) and $\mathbf{J}_{\text{total}} = 0$) is

$$\nabla^2 \mathbf{E} - \epsilon_c \ddot{\mathbf{E}} = 0, \quad (17)$$

i.e. not a real equation in real unknowns; a point whose significance might be missed if expecting to take the real part.

Using a *Narrowband Approximation* we can recover the correct physical behaviour, although when solving the dispersion (2) one needs to be careful about the square root. We choose ω, k in (1) to satisfy the dispersion relation

$$k c_0 - \tilde{n}(-\omega) \omega = 0, \quad (18)$$

and consider all relevant frequencies. With an over-bar denoting complex conjugates, the associated solutions are created by substituting $\omega \rightarrow \pm\omega, \omega \rightarrow \pm\bar{\omega}, k \rightarrow \pm k, \text{ and } k \rightarrow \pm\bar{k}$. Then, combining (2) and (3) gives $c_0^2 k^2 - \omega^2 \tilde{n}(-\omega)^2 = 0$. The eight roots of this and its complex conjugate are given by

$$E_x = \exp(-i\omega t \pm ikz) \quad \text{satisfies} \quad \tilde{n}(-\omega) \omega = \pm c_0 k, \quad (19)$$

$$E_x = \exp(i\omega t \mp ikz) \quad \text{satisfies} \quad \tilde{n}(\omega) \omega = \pm c_0 k, \quad (20)$$

$$E_x = \exp(-i\bar{\omega} t \pm i\bar{k}z) \quad \text{satisfies} \quad \overline{\tilde{n}(\omega)} \bar{\omega} = \pm c_0 \bar{k}, \quad (21)$$

$$E_x = \exp(i\bar{\omega} t \mp i\bar{k}z) \quad \text{satisfies} \quad \tilde{n}(\bar{\omega}) \bar{\omega} = \pm c_0 \bar{k}, \quad (22)$$

(see Supplementary Material) which uses $\tilde{n}(-\bar{\omega}) = \overline{\tilde{n}(\omega)}$, a consequence of the reality condition on \tilde{n} .

Now, if we apply the NBA, we know that all the fields are concentrated about two modes, i.e. at $\omega \approx \omega_0$ and $\omega \approx \bar{\omega}_0$.

Let $N = \tilde{n}(-\omega_0)$, so that for $\omega \approx \omega_0$ we have $\tilde{n}(-\omega) \approx N$. Similarly, we also have $\bar{N} = \tilde{n}(-\bar{\omega}_0)$.

To obtain a real $E_x(t, z)$ we need to add the complex conjugate. As $\text{Im}(\omega_0) = \text{Im}(-\bar{\omega}_0)$ we construct the total field from (19) and (22) above to give

$$\begin{aligned} E_x(t, z) &= g_+^- e^{-i\omega t + ikz} + g_-^- e^{-i\omega t - ikz} \\ &\quad + g_+^+ e^{i\bar{\omega} t - i\bar{k}z} + g_+^+ e^{i\bar{\omega} t + i\bar{k}z}. \end{aligned} \quad (23)$$

We are now in a position to reconsider our time boundary system in the context of dispersive media. Before the time boundary $t < t_b = 0$ we have the vacuum. Assuming a narrowband initial pulse enveloping the single mode (10), where $\omega_a = c_0 k_a \in \mathbb{R}$, and $k_a > 0$. Whichever TBC we assume we obtain $k_c = \pm k_a$. Again the choice of root is unimportant, therefore we set $k_c = k_a$, so that $k_c > 0$. After the time boundary, we have dispersion relations given by (19)–(22). In order to obtain the physical solutions consistent with $k_c > 0$ we choose $\text{Re}(N) > 0, \text{Im}(N) > 0$ and the modes given by (19) and (22). For convenience we define a wave speed $C = C_R + i C_I = c_0 / N$, where $C_R, C_I \in \mathbb{R}, C_R > 0$ and $C_I < 0$. From (23) we have,

$$E_x(t, z) = E_0 e^{k C_I t} \left(\frac{N+1}{N+\bar{N}} e^{-ik(C_R t - z)} + \frac{\bar{N}+1}{N+\bar{N}} e^{-ik(C_R t + z)} \right) \quad (24)$$

where $k = k_c > 0$ (see Supplementary Material), and the EM field remains real and damped. However, we no longer have a single differential equation (17), as we now need two:

$$\begin{cases} \nabla^2 \mathbf{E} - N \ddot{\mathbf{E}} = 0 & \text{for frequencies } \omega \approx \omega_0 \text{ in } \mathbf{E}, \\ \nabla^2 \mathbf{E} - \bar{N} \ddot{\mathbf{E}} = 0 & \text{for frequencies } \omega \approx \bar{\omega}_0 \text{ in } \mathbf{E}. \end{cases} \quad (25)$$

Thus by using the NBA and allowing dispersion, we can match the TBC, and obtain a physical, dampened, real-valued solution for the electric field; but this does require two post-boundary refractive indices (i.e. N and \bar{N}), not one.

Dynamic Material Models: It is not possible to both implement a physically consistent time boundary with a constant complex ϵ_c , and escape the requirement for the NBA in (25). This means we must instead use an explicitly causal [30] dynamic response model for the medium, thus providing fully dispersive CR. Since a response model adds extra field(s) to describe the material response, the coupled EM-material system will both have more than two modes and need ABCs.

A minimal but sufficient material response given by is

$$\mathbf{D} = \epsilon_0 \mathbf{E} + \mathbf{P} \quad \text{where} \quad \dot{\mathbf{P}} = -\lambda \mathbf{P} + \chi_0 \mathbf{E}, \quad (26)$$

so that in the steady state $\mathbf{P} = \chi_0 \lambda^{-1} \mathbf{E}$. In this model, as long as the loss λ is large compared to the field frequency, with the desired change in permittivity $\Delta\epsilon = \chi_0 / \lambda$ held fixed, it indeed responds as if it were a medium of complex constant CR. This model also requires a boundary condition for the dielectric polarization \mathbf{P} field, namely $[\mathbf{P}] = 0$. The polarization field (26) is related to a bound current $\mathbf{J}_b = \dot{\mathbf{P}} = -\lambda \mathbf{P} + \chi_0 \mathbf{E}$. This \mathbf{J}_b is driven by, and hence indirectly damps, the field

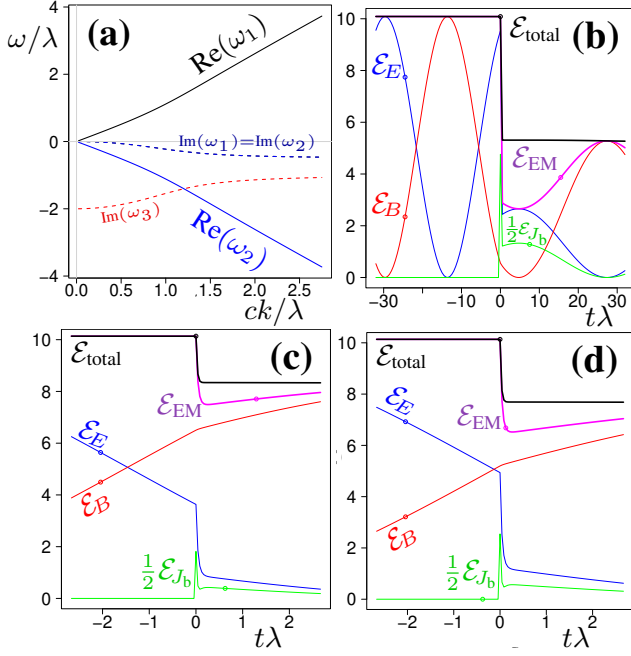


FIG. 2: (a) The dispersion relation (28) for the simple material response model of (26), where $\chi_0 = \epsilon_0 \lambda$ and real k . The two propagating solutions $\omega_1, \omega_2 \in \mathbb{C}$ have the same small damping, while the third $\omega_3 \in i\mathbb{R}$ is pure loss. In (b,c,d) we see what happens as the system crosses a time boundary at $t = 0$ between vacuum $\chi_0 = 0$ and $\chi_0 = \epsilon_0 \lambda$; where (c,d) show a narrower range of t around $t = 0$. The different initial conditions used in (b,c,d) demonstrate the timing-sensitive behaviour caused by the boundary. These graphs compare the energies in the three fields $\mathcal{E}_E = \epsilon_0 E^2$, $\mathcal{E}_B = B^2/\mu_0$ and $\mathcal{E}_{J_b} = J_b^2/(\chi_0 \lambda)$; but we show $\frac{1}{2} \mathcal{E}_{J_b}$ to increase visibility. Total energy is conserved for $t < 0$; but just after the time boundary, \mathcal{E}_E (and hence \mathcal{E}_{EM}) rapidly reduce as excitation is transferred to J_b , where it is strongly damped. The energy lost though J_b depends on how strongly it is driven by E until the new dynamic near-equilibrium is reached. Direct damping from the lossy ω_3 solution is shown by rapid decay of \mathcal{E}_{J_b} just after the transition, after which further loss of energy is small and is proportional to ω/λ .

E ; and our simulation results shown in figure 2 use this J_b approach. Used after the time boundary ($t > t_b$), this medium has a dispersive behaviour given by

$$\tilde{\epsilon}(-\omega) = \epsilon_0 + \frac{\chi_0}{\lambda - i\omega}, \quad (27)$$

where $\chi_0 > 0$ and $\lambda > 0$; and the steady state is reached when $\omega/\lambda \rightarrow 0$. The resulting cubic dispersion relation is

$$\epsilon_0 \mu_0 (\lambda - i\omega) \omega^2 + \mu_0 \chi_0 \omega^2 - k^2 (\lambda - i\omega) = 0. \quad (28)$$

This equation in ω and fixed k^2 produces three solutions as opposed to the two given in (11) or (24). Since (28) has real coefficients when written as a polynomial in $(i\omega)$, and as a cubic has at most two non-real roots for $i\omega$, the three solutions consist of a complex conjugate pair and a real valued one. The pair correspond to counter propagating waves (modes) with the same damping, with the other solution (mode) being non-propagating and purely damped (see figure 2(a)).

At a time boundary where $k \in \mathbb{R}$ and $k > 0$, we have three outgoing modes, requiring three boundary conditions. Two TBC are given by either the natural (8) or fundamental (9) TBC (7); the ABC of course is just the $[\mathbf{P}] = 0$ evident from the dynamic model (26). This ABC is analogous to the Pekar ABC [31], which are required when an EM wave passes into a spatially dispersive medium.

Simulation results are shown in figure 2(b,c,d), demonstrating the system behaviour as it passes the boundary. Despite the excellent match to a medium with constant complex CR before and sufficiently far after the boundary transition, it does not exhibit the unphysical behaviour of prescribed constant complex CRs. Instead, just after $t = t_b = 0$ in figures 2(c,d) we can see a rapid rebalancing as E and J_b (i.e. \mathbf{P}) adjust to the recently changed χ_0 . Note also the slight overshoot in \mathcal{E}_J just after the boundary, due to the dampened ω_3 . These occur on a timescale set by λ , and incur an E dependent energy loss.

In Conclusion, we have shown that even simple time boundaries in optics cannot be described by the standard “constant complex permittivity” model. Only with a dynamic or dispersive model of the propagation medium can physical results be predicted. This is despite the fact that a constant complex permittivity model works for spatial boundaries; but then damping is a *time-dependent* phenomenon, not a spatial one. This conclusion is supported by NBA calculations and time domain simulations, and has implications for the many types of systems with temporal boundaries. These effects may be particularly relevant for the propagation of relativistically intense electromagnetic waves in plasma; e.g. for example, in the wakefield accelerator in the bubble regime, or for relativistically induced transparency in laser-solid interactions. Further, our conclusions are easily generalized to other wave systems.

It is arguably unsurprising that a good model of a time boundary requires a model that can admit non-trivial time dependence, i.e. either a time domain response model or a frequency domain dispersion. Time boundaries are a temporal, dynamic phenomena, and need to be treated as such.

Acknowledgments: Both JG and PK are grateful for the support provided by STFC (Cockcroft Institute, ST/G008248/1 and ST/P002056/1). DAJ, JG, and PK acknowledge support from the EPSRC (Lab in a Bubble, EP/N028694/1). DAJ acknowledges funding from the European Union’s Horizon 2020 research and innovation programme under grant agreement no. 871124 Laserlab-Europe. RS would like to thank AFOSR (FA8655-20-1-7002) for support. PK would also like to acknowledge recent support from the UK National Quantum Hub for Imaging (QUANTIC, EP/T00097X/1).

* <https://orcid.org/0000-0003-1597-6084>

† <https://orcid.org/0000-0001-8728-1463>

‡ <https://orcid.org/0000-0001-5744-8146>

§ <https://orcid.org/0000-0002-3006-5492>

[1] F. R. Morgenthaler,

- IRS Trans. Microwave Theory and Techniques **6**, 167 (1958), doi:10.1109/TMTT.1958.1124533.
- [2] M. Kolesik and J. V. Moloney, Phys. Rev. E **70**, 036604 (2004), doi:10.1103/PhysRevE.70.036604.
- [3] Y. Mizuta, M. Nagasawa, M. Ohtani, and M. Yamashita, Phys. Rev. A **72**, 063802 (2005), doi:10.1103/PhysRevA.72.063802.
- [4] G. Genty, P. Kinsler, B. Kibler, and J. M. Dudley, Opt. Express **15**, 5382 (2007), doi:10.1364/OE.15.005382.
- [5] P. Kinsler, J. Opt. **20**, 025502 (2018), doi:10.1088/2040-8986/aaa0fc, arXiv:1501.05569.
- [6] P. Kinsler, J. Phys. Commun. **2**, 025011 (2018), doi:10.1088/2399-6528/aaa85c, arXiv:1202.0714.
- [7] J. de Rosny and M. Fink, Phys. Rev. Lett. **89**, 124301 (2002), doi:10.1103/PhysRevLett.89.124301.
- [8] Y. Kiasat, V. Pacheco-Pena, B. Edwards, and N. Engheta (Conference on Lasers and Electro-Optics, Science and Innovations, San Jose, California, United States, 2018), p. JW2A.90, ISBN 978-1-943580-42-2.
- [9] J. P. Turpin, J. A. Bossard, K. L. Morgan, D. H. Werner, and P. L. Werner, Intl. Journal of Antennas and Propagation **2014**, 429837 (2014), doi:10.1155/2014/429837.
- [10] M. McCall, J. B. Pendry, V. Galdi, Y. Lai, S. A. R. Horsley, J. Li, J. Zhu, R. C. Mitchell-Thomas, O. Quevedo-Teruel, P. Tassin, et al., J. Opt. **20**, 063001 (2018), doi:10.1088/2040-8986/aab976.
- [11] M. W. McCall, A. Favaro, P. Kinsler, and A. Boardman, J. Opt. **13**, 024003 (2011), doi:10.1088/2040-8978/13/2/024003.
- [12] J. Gratus, P. Kinsler, M. W. McCall, and R. T. Thompson, New J. Phys. **18**, 123010 (2016), doi:10.1088/1367-2630/18/12/123010, arXiv:1608.00496.
- [13] P. Kinsler and M. W. McCall, Ann. Phys. (Berlin) **526**, 51 (2014), doi:10.1002/andp.201300164, arXiv:1308.3358.
- [14] P. Kinsler and M. W. McCall, Phys. Rev. A **89**, 063818 (2014), doi:10.1103/PhysRevA.89.063818, arXiv:1311.2287.
- [15] K. Sacha and J. Zakrzewski, Reports on Progress in Physics **81**, 016401 (2018), doi:10.1088/1361-6633/aa8b38, arXiv:1704.03735.
- [16] G. W. Milton and O. Mattei, Proc. Royal Soc. A **473**, 20160819 (2017), doi:10.1098/rspa.2016.0819, arXiv:1611.06257.
- [17] J. B. Pendry, Phys. Rev. Lett. **85**, 3966 (2000), https://doi.org/10.1103/PhysRevLett.85.3966.
- [18] L. S. Dolin, Izv. Vyssh. Uchebn. Zaved. Radiofizika **4**, 964 (1961), https://www.math.utah.edu/~milton/DolinTrans2.pdf.
- [19] P. Kinsler and M. W. McCall, Microwave Opt. Techn. Lett. **50**, 1804 (2008), doi:10.1002/mop.23489, arXiv:0806.1676.
- [20] B. Chen, B. Gao, C. Ge, and J. Li, Modern Applied Sciences **3**, 68 (2009), doi:10.5539/mas.v3n10p68.
- [21] B. Chen and X. Lu, Modern Applied Sciences **5**, 243 (2011), doi:10.5539/mas.v5n4p243.
- [22] A. H. D. Cheng and D. T. Cheng, Engineering Analysis with Boundary Elements **29**, 268 (2005), doi:10.1016/j.enganabound.2004.12.001.
- [23] J. Gratus, P. Kinsler, and M. W. McCall, Eur. J. Phys. **40**, 025203 (2019), arXiv:1903.01957, doi:10.1088/1361-6404/ab009c.
- [24] J. Gratus, P. Kinsler, and M. W. McCall, Found. Phys. **49**, 330 (2019), doi:10.1007/s10701-019-00251-5, arXiv:1904.04103.
- [25] J. Gratus, M. W. McCall, and P. Kinsler, Phys. Rev. A **101**, 043804 (2020), arXiv:1911.12631, doi:10.1103/PhysRevA.101.043804.
- [26] B. Nistad and J. Skaar, Phys. Rev. E **78**, 036603 (2008), doi:10.1103/PhysRevE.78.036603.
- [27] P. Kinsler, Phys. Rev. A **79**, 023839 (2009), doi:10.1103/PhysRevA.79.023839, arXiv:0901.2466.
- [28] E. Feigenbaum, N. Kaminski, and M. Orenstein, Opt. Express **17**, 18934 (2009), doi:10.1364/OE.17.018934.
- [29] P. Kinsler (2014), arXiv:1408.0128.
- [30] P. Kinsler, Eur. J. Phys. **32**, 1687 (2011), doi:10.1088/0143-0807/32/6/022, arXiv:1106.1792.
- [31] S. I. Pekar, Zh. Eksp. Teor. Fiz **34**, 1176 (1958), http://www.jetp.ac.ru/cgi-bin/e/index/e/7/5/p813?a=list.
- [32] A. D. Boardman, N. King, and L. Velasco, Electromagnetics **25**, 365 (2005), doi:10.1080/02726340590957371.
- [33] A. Schuster, *An introduction to the theory of optics* (Edward Arnold, London, 1904).

Supplementary Material

In Linear Media – spatial evanescence

Lemma 1. *Given that for $\omega \in \mathbb{R}$, $\omega > 0$ plane waves are spatially evanescent in the propagation direction then $\text{Im}(\tilde{\epsilon}(-\omega)) > 0$.*

Proof. Given (1) with $\omega > 0$. For $\text{Re}(k) > 0$ then the direction of propagation is positive z . If the plane waves are evanescent for positive z then $\text{Re}(ikz) < 0$ hence $\text{Im}(k) > 0$. This implies k lies in the top right quadrant of \mathbb{C} . Hence $\text{Im}(k^2) > 0$.

Likewise for $\text{Re}(k) < 0$ then the direction of propagation is negative z . If the plane waves are evanescent for negative z then $\text{Re}(ikz) < 0$ hence $\text{Im}(k) < 0$. This implies k lies in the bottom left quadrant of \mathbb{C} . Hence $\text{Im}(k^2) > 0$.

In both cases $\text{Im}(k^2) > 0$ and since $\omega^2 > 0$ then (2) implies $\text{Im}(\tilde{\epsilon}(-\omega)) > 0$. \square

In Linear Media – a note on negative refractive index

From (3), $\text{Im}(\tilde{\epsilon}(-\omega)) > 0$ implies that $\tilde{n}(-\omega)$ is either (a) in the top right quadrant of the complex plane $\{\text{Re}(\tilde{n}) > 0 \text{ and } \text{Im}(\tilde{n}) > 0\}$, or (b) in the bottom left quadrant $\{\text{Re}(\tilde{n}) < 0 \text{ and } \text{Im}(\tilde{n}) < 0\}$. Consequently, having $\text{Re}(\tilde{n}(-\omega)) < 0$ does not contradict our assumption that the real part of both permittivity and permeability are positive: it is still possible to have a negative index of refraction [32, 33].

Using a Narrowband Approximation – the eight roots

Demonstration of (19)-(22). Since we chose (1) to satisfy (18) then this is (19) for $E_x = \exp(-i\omega t + ikz)$. Replacing $k \rightarrow -k$ then gives (19).

Replacing $\omega \rightarrow -\omega$ and $k \rightarrow -k$ then gives (21).

Taking the complex conjugate of (19) and using $\tilde{n}(-\bar{\omega}) = \overline{\tilde{n}(\omega)}$ gives (22).

Replacing $\omega \rightarrow -\omega$ and $k \rightarrow -k$ in (22) then gives (21). \square

Using a Narrowband Approximation – proof

Proof of (24). From (23) we have

$$\begin{aligned} B_y(t, z) &= \frac{e^{kC_1 t}}{C_1 - iC_R} \left(g_-^- e^{-ik(C_R t - z)} - g_-^- e^{-ik(C_R t + z)} \right) \\ &\quad + \frac{e^{kC_1 t}}{C_1 + iC_R} \left(g_-^+ e^{ik(C_R t - z)} - g_+^+ e^{ik(C_R t + z)} \right) \\ &= \frac{\bar{N} e^{kC_1 t}}{c_0} \left(g_+^- e^{-ik(C_R t - z)} - g_-^- e^{-ik(C_R t + z)} \right) \\ &\quad + \frac{N e^{kC_1 t}}{c_0} \left(g_-^+ e^{ik(C_R t - z)} - g_+^+ e^{ik(C_R t + z)} \right) \end{aligned} \quad (29)$$

Using the fundamental TBC (9) we get for $t = 0^+$ and $k \in \mathbb{R}$

$$\begin{aligned} E_x(0^+, z) &= e^{ikz} (g_+^- + g_+^+) + e^{-ikz} (g_-^- + g_-^+) \\ c_0 B_y(0^+, z) &= e^{ikz} (\bar{N} g_+^- - N g_+^+) + e^{-ikz} (N g_-^+ - \bar{N} g_-^-) \end{aligned}$$

and hence

$$g_+^- = \overline{g_+^+} = \frac{E_0}{2} \frac{N+1}{N+\bar{N}} \quad \text{and} \quad g_-^- = \overline{g_-^+} = \frac{E_0}{2} \frac{\bar{N}+1}{N+\bar{N}}$$

Substituting into (23) gives (24). \square

Dynamic Material Models – applicability of the minimal model

This model (i.e. (26)), being defined by a temporal differential equation, is necessarily explicitly causal [30]. It works as intended when (i) the desired positive permittivity shift $\chi_0 > 0$, and when (ii) $\chi_0/\lambda\epsilon_0 \lesssim 3$. In this regime the polarization (or microscopic polarization current) is adiabatically slaved to the phase of electric field, and so accurately models the desired effective permittivity; indeed the effective loss at low frequencies is proportional to ω/λ , i.e. increasing the polarization current loss λ actually *reduces* the effective damping in the CW limit.

If the first condition does not hold, a positive polarization can have a negative energy; thus the amplitudes of \mathbf{E} and \mathbf{P} can increase without limit whilst still conserving energy.

If the parameters change so that the second condition starts to fail, the three modes – two electromagnetic and one polarization – become ever more strongly coupled and eventually exhibit a complicated dynamics (and dispersion) not relevant to our presentation here.

Dynamic Material Models – beyond the minimal model

A more general constitutive relationship would be combine a set of Lorentz oscillators. Working in the time domain, we would have $\mathbf{D} = \epsilon_0 \mathbf{E} + \sum_s \mathbf{P}_s$ where $\dot{\mathbf{P}}_s + \lambda_s \mathbf{P}_s + \alpha_s \mathbf{P}_s = \chi_s \mathbf{E}$ and the $2s_{\max}$ natural ABCs are $[\mathbf{P}_s] = 0$ and $[\dot{\mathbf{P}}_s] = 0$, where s_{\max} indexes the set of oscillators. Here χ_s is the coupling, λ_s is the damping, and α_s the natural frequency of the oscillator.

In the frequency domain, this has the dispersion

$$\tilde{\epsilon}(-\omega) = \epsilon_0 + \sum_{s=1}^{s_{\max}} \frac{\chi_s}{-\omega^2 - i\lambda_s \omega + \alpha_s^2}. \quad (30)$$

Expanding out the dispersion relation (2) leads to a polynomial in ω of degree $(2s_{\max} + 2)$. Generating $(2s_{\max} + 2)$ modes which in general will be propagating, meaning we need to derive $2s_{\max}$ ABCs.

Remarks – Causality, dispersion, and the NBA

Across our time boundary, a change in constant complex CR for a medium is just an instantaneous change, which is straightforwardly causal. Causal behaviour, however, of itself is not necessarily guaranteed to give physically reasonable predictions. Indeed, all but one of the results in this paper are causal – even the unphysical (17), where the future behaviour is by construction explicitly dependent on the past behaviour. The single exception is the narrowband result (25), because under this approximation questions of causality are moot.

Causality is often tested by applying the Kramers-Kronig relations (see e.g. [30]), but they do not apply to all situations.

For example, even though the result (16) is causal, and clearly so when solving in the time domain, as an exponentially increasing function it cannot be Fourier transformed so as to allow Kramers-Kronig to be tested. Indeed, since the original function of Kramers-Kronig was to analyse, test, or correct raw data *collected* in the frequency domain, using them as a causality test when a time domain description is already available is redundant.

This is why the dynamical model (26) is a natural starting point for an examination of temporal boundaries; although of course more complicated models, such as the summed Lorentzians of (30), or ones involving (causal) integral kernels, can be constructed. Notably, even the highly simplified (26), designed to give results that in the appropriate limit are as close as possible to the failed constant complex CR model, is sufficient to restore physical behaviour.

Remarks – CR and Ohmic losses

Ohmic losses are also covered by our analysis; as they can also be modelled by a complex permittivity. Since the polarisation corresponding to ohmic losses is given by $\mathbf{P} = (\sigma/(-i\omega))\mathbf{E}$ then this is an alternative dispersive constitutive relation, which means it does not contradict the statements about constant ϵ_c .